Electronic Supplementary Material (ESI) for Journal of Materials Chemistry A.
This journal is © The Royal Society of Chemistry 2019

Supporting Information

For

Co-regulating Surface and Bulk Structure of Li-Rich Layered Oxide by Phosphor Doping Strategy for High-Energy Li-Ion Battery

Min-Jun Wang [1], Fu-Da Yu [1]*, Gang Sun [1], Jian Wnag[2], Ji-Gang Zhou [2], Da-Ming Gu [1], Zhen-Bo Wang [1]*

[1] MIIT Key Laboratory of Critical Materials Technology for New Energy Conversion and Storage, School of Chemistry and Chemical Engineering, Harbin Institute of Technology, No. 92 West-Da Zhi Street, Harbin, 150001, China

[2] Canadian Light Source Inc., Saskatoon, SK S7N 2V3, Canada

* Corresponding author. Tel.: +86-451-86417853; Fax: +86-451-86418616. E-mail: yufuda@hit.edu.cn (F. D. Yu); wangzhb@hit.edu.cn (Z. B. Wang)

Synthesis method

The material of $Li[Li_{0.2}Ni_{0.133}Co_{0.133}Mn_{0.534}]O_2$ was synthesized by a typical co-precipitation method. 2 mol L^{-1} aqueous solution of $CoSO_4 \cdot 7H_2O$, $NiSO_4 \cdot 6H_2O$ and $MnSO_4 \cdot H_2O$ with appropriate molar ratios was added into a continuously stirred tank reactor at the temperature of 55 ^oC. In the meantime, an equimolar Na_2CO_3 solution with desired amount of NH_4OH was added into the reactor to keep the pH at 7.50. The coprecipitated particles were collected and dried at 120 ^oC for 24 h. The obtained precursor particles were mixed with precalculated Li_2CO_3. 3% excess of lithium was introduced intentionally to compensate the Li loss during the calcination. The mixture was first annealed at 450 ^oC for 3 h and then at 800 ^oC for 12 h.

Electrochemical Measurements

Cathode electrodes were prepared by mixing active material, acetylene black, polyvinylidene difluoride and appropriate quantity of N-methyl pyrrolidone (NMP) solvent homogeneously and pasting the mixture on an aluminium foil. Then the aluminium foil was dried at 120 ^oC for 12 h to remove the NMP solvent. After that, the electrode sheets were punched into circular disks as cathode. The loading mass of the active material was approximately 4.0 mg cm^{-2}.

The coin-type cells were assembled in an argon-filled dry glove-box using lithium metal as anode. The composition of electrolyte consists of 1 M $LiPF_6$ dissolved in ethylene carbonate, dimethyl carbonate and diethyl carbonate at a volumetric ratio of 1:1:1. A NEWARE battery tester was used for Galvanostatic charge–discharge experiments and GITT tests at the temperature of 25 ^oC. During GITT testing, a constant current flux of 40 mA g^{-1} for a given time period (10 min) was supplied, followed by an open circuit conditions for 40 min. EIS and cyclic voltammetry (CV) were measured by an electrochemical workstation (CHI660E). EIS was recorded by applying an AC voltage of 5 mV in the frequency range from 10^5 Hz to 10^{-2} Hz. The C-rates mentioned in this text were calculated considering 1 C as 250 mA g^{-1}.

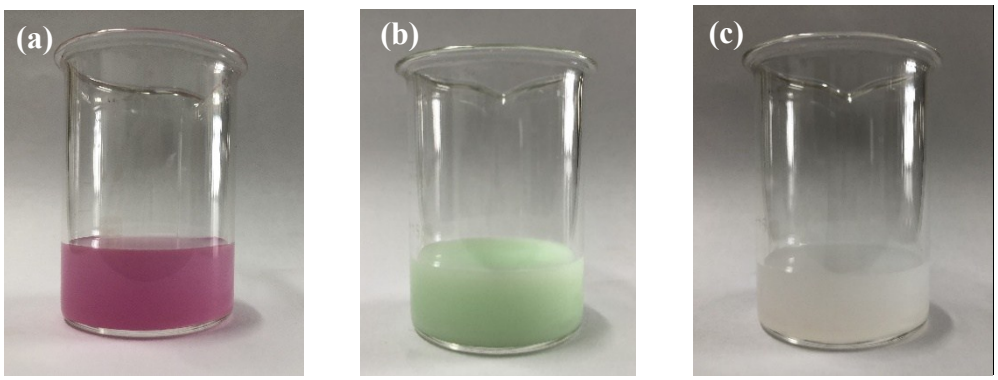

Fig. S1 The precipitation of (a) $Co_2P_2O_7$, (b) $Ni_2P_2O_7$ and (c) $Mn_2P_2O_7$.

The aqueous solution of sodium pyrophosphate can react with transition metal ions (Co^{2+}, Ni^{2+}, Mn^{2+}). The reaction equation is depicted in the following:

$2Co^{2+}+P_2O_7^{4-}\rightarrow Co_2P_2O_7\downarrow$

$2Ni^{2+}+P_2O_7^{4-}\rightarrow Ni_2P_2O_7\downarrow$

$2Mn^{2+}+P_2O_7^{4-}\rightarrow Mn_2P_2O_7\downarrow$

The precipitation coefficient of pyrophosphate is a little smaller than carbonate. The precipitation is displayed in Figure S1.

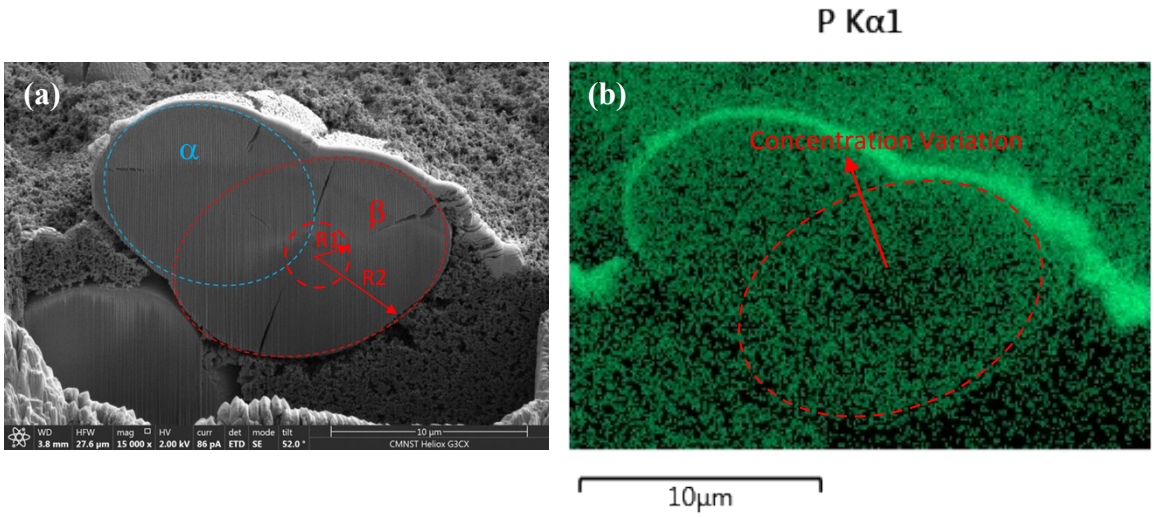

Fig. S2 SEM and mapping of cross-section of phosphor doped precursor.

From the shape of cross-section in Fig. S1a, the particle is combined by two secondary particles, α and β. Particle β is bigger than particles α, which indicates particle β is generated earlier than particles α. Due to the stable concentration of phosphorus element in particle α, particle α must be originated from stage 4 of Fig. 1a.

In order to simplify calculating, we take the particles β to be spheres. Therefore, the computational formula of volume is:

$$V = \frac{4}{3}\pi r^3$$

V presents the volume and r is the radius.

R1 is the radius of section with phosphor concentration variation. R2 is the radius of particle β. From the DES test and SEM of cross-section in Fig 1, the R1 is about 2μm and R2 is 5-7μm.

$$\frac{V_1}{V_2} = \frac{\frac{4}{3}\pi {R_1}^3}{\frac{4}{3}\pi {R_2}^3} = \frac{2*2*2}{5*5*5} = 6.4\%$$

V_1 is the volume with phosphor concentration variation. V_2 is the volume of particle β.

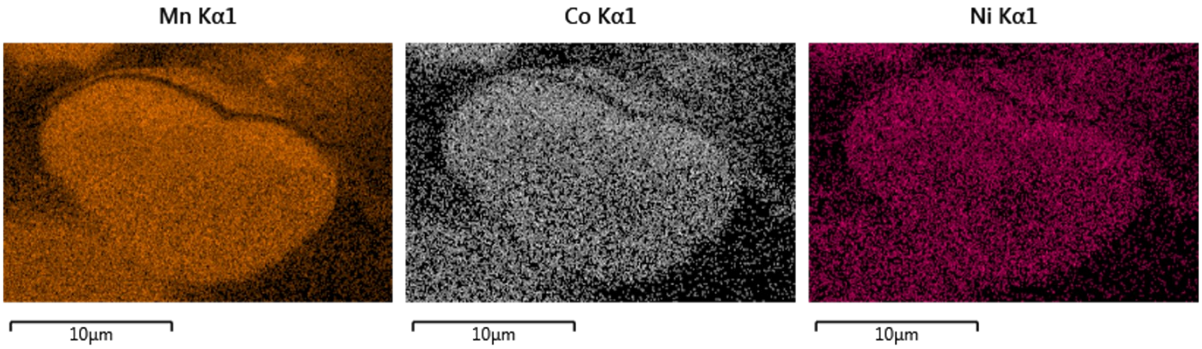

Fig. S3 Mapping image of cross-section of phosphor doped precursor.

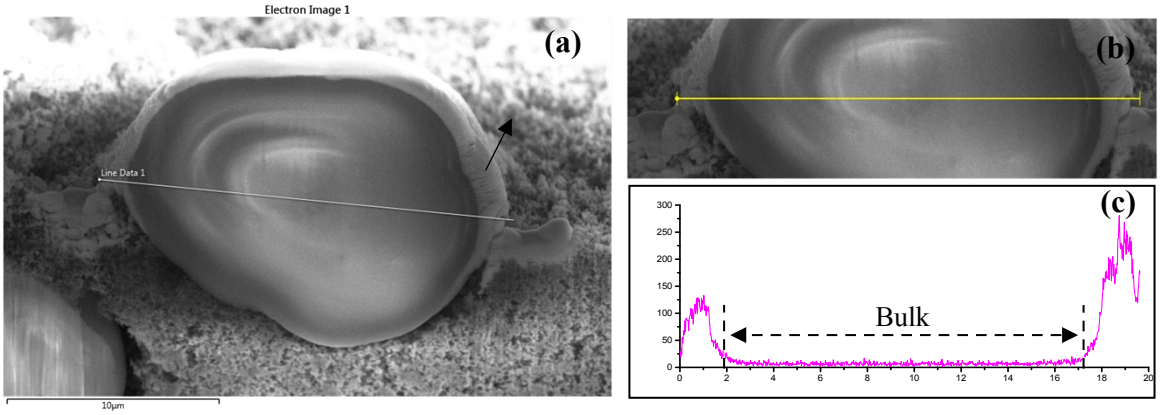

Fig. S4 The cross-section of normal sample's precursor and EDS line scan.

Due to the binder in the particle surface, high intensity of phosphorus content is detected in the range of 0-2 and 17-20 in Fig S3c. In the bulk of normal sample (2-17), there is no obvious phosphorus element existent.

Table 1 Relative amounts of Co, Mn, and Ni (ICP data).

	Ni	Co	Mn
NM-LRM	0.1666	0.1685	0.6648
PD-LRM	0.1680	0.1715	0.6605

The ICP date is depicted to demonstrate the impact of phosphor doping on the metal element content. From the IPC data, the content of Mn is decreased a little and the content of Ni and Co is increased after phosphor doping.

Table S2. Summary of structural refinement of the NM-LRM and PD-LRM samples by Rietveld method.

Samples	a=b	c	c/a	intermixing of cations
NM-LRM	2.8521(7)	14.2237(0)	4.987	2.84%
PD-LRM	2.8540(2)	14.2473(4)	4.992	0.79%

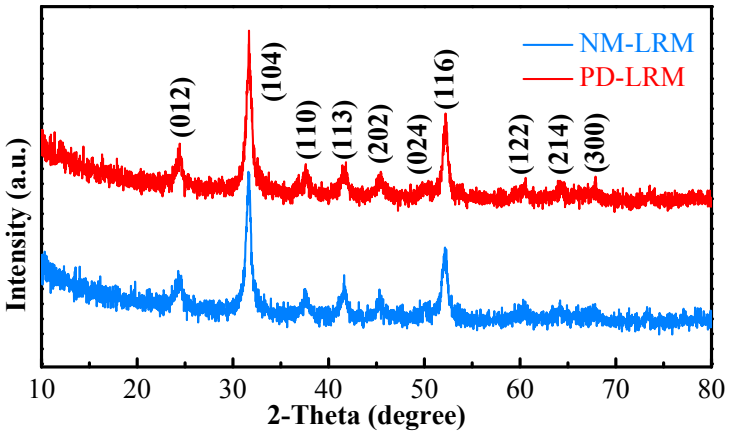

Fig. S5 The XRD patterns of normal and phosphorus doped precursors.

The XRD patterns of normal and phosphorus doped precursors are quite similar, indicating the using of $Na_4P_2O_7$ as an auxiliary precipitant do not have distinct effect on the precursor crystal structure. Besides, there are no evident peak of $M_2P_2O_7$ (M=Ni, Co, and Mn) found in the XRD pattern, which must be due to the low content and poor crystallinity.

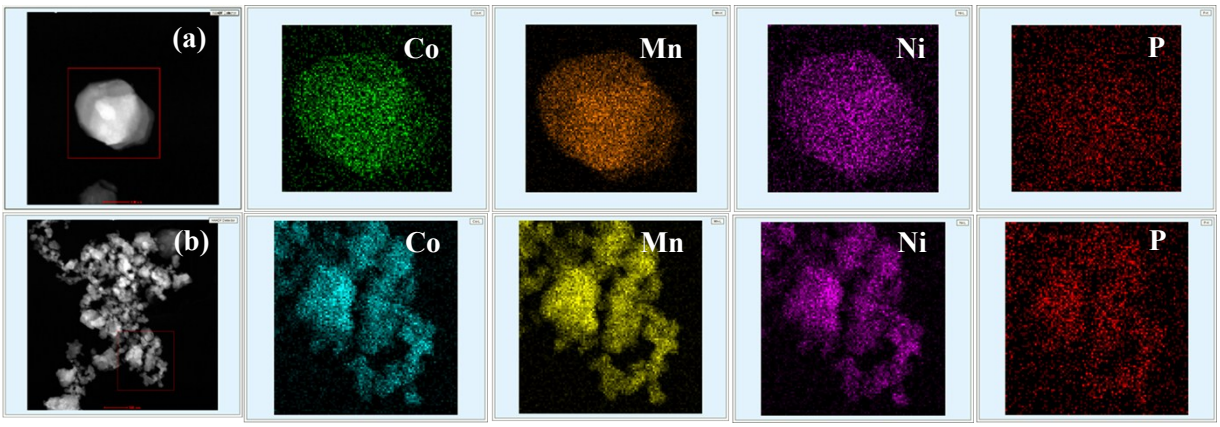

Fig. S6 TEM mapping images of the (a) NM-LRM and (b) PD-LRM samples.

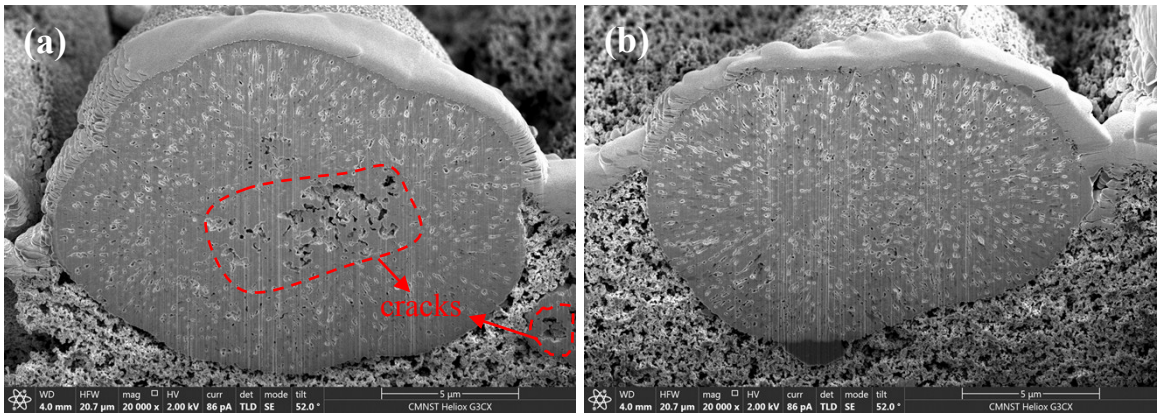

Fig. S7 The cross-section of (a) NM-LRM and (b) PD-LRM samples.

Table S3. The tap density of NM-LRM and PD-LRM samples.

Samples	NM-LRM	PD-LRM
Tap density (g cm^{-3})	1.93	2.14

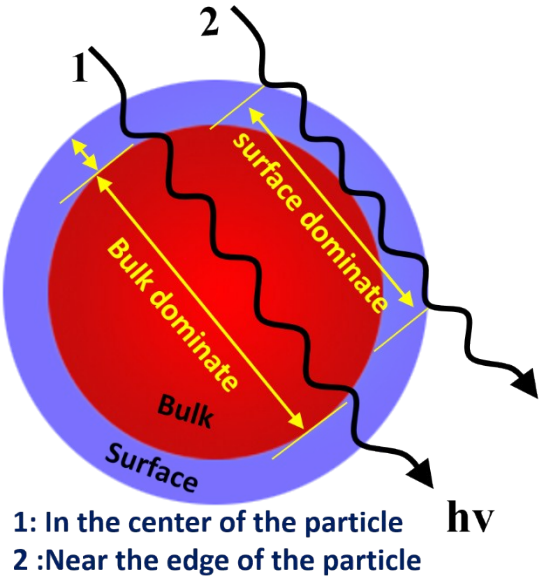

Fig. S8 Schematic illustration of the measurement method.

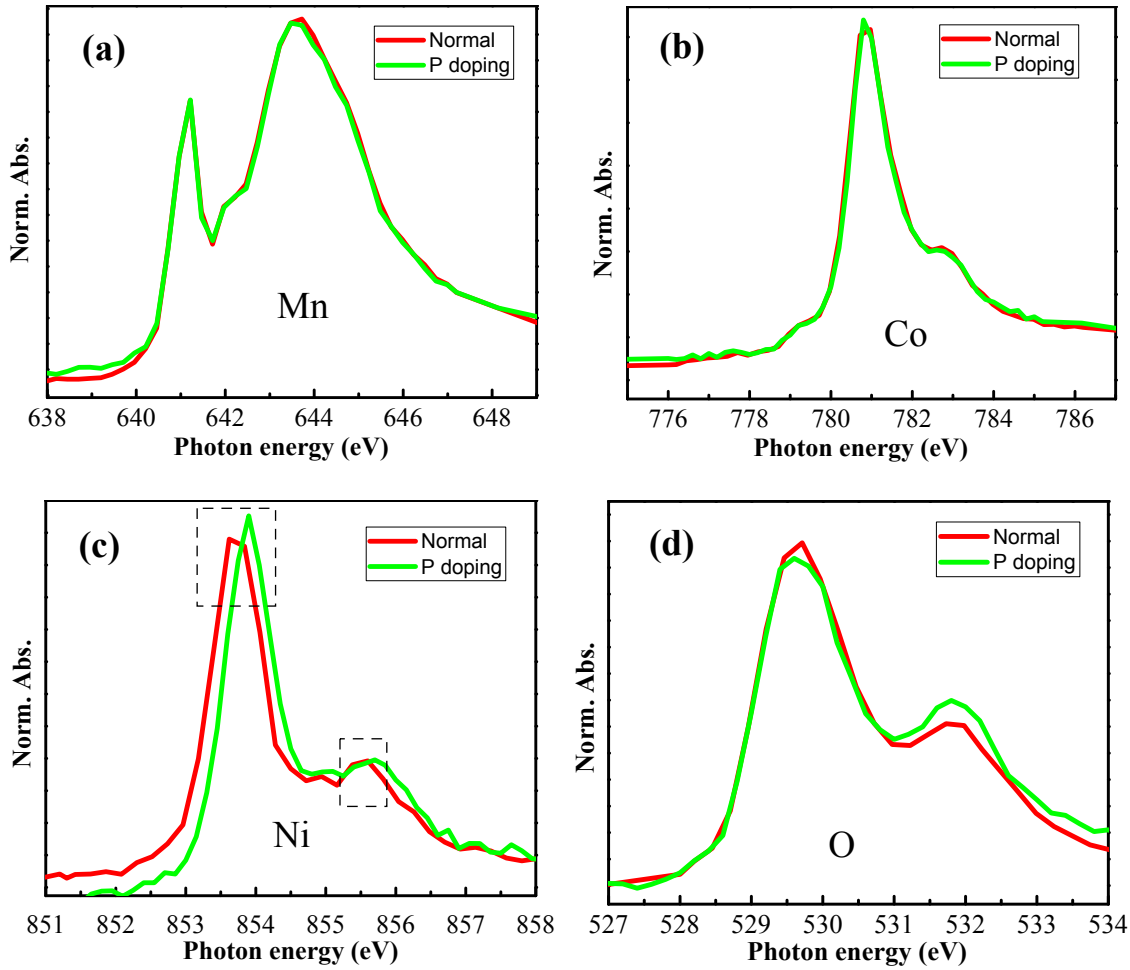

Fig. S9 The surface XANES spectra of (a) Mn, (b) Co, (c) Ni, and (d) O of the two samples.

For clarity, the surface spectra of same elements are compared and presented in Fig. S4. The surface spectra of Mn and Co in both the two samples are well overlapped and the valence states can be assigned to Mn^{4+} and Co^{3+}. Those imply that phosphor doping has trifle impact on the surface chemical state of Mn and Co.

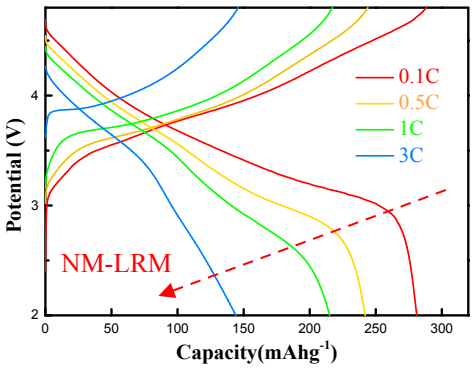

Fig. S10 Charge/discharge profiles at different rates (0.1–3C) for NM-LRM.

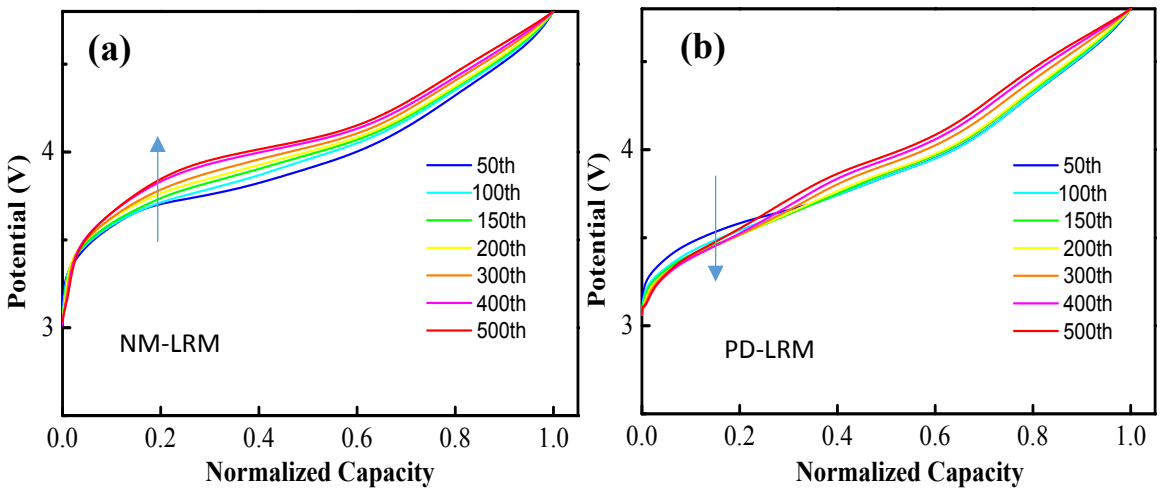

Fig. S11 Charge profiles of (a) NM-LRM and (b) PD-LRM samples at different cycles.

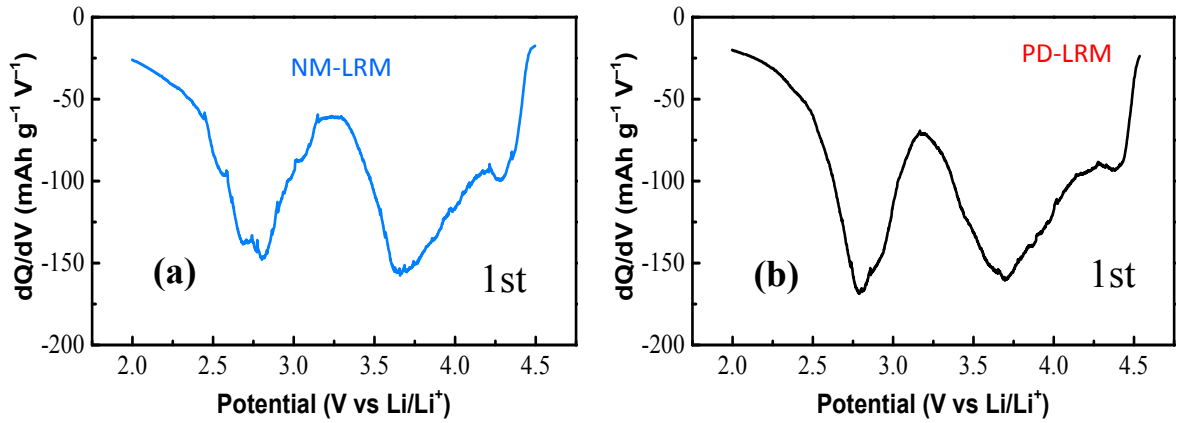

Fig. S12 The dQ/dV curves of (a) NM-LRM and (b) PD-LRM samples at first discharge process at 1C after activation.

The Calculation Method of Diffusion Coefficient.

The Li-ion diffusion coefficient (D^{Li^+}) is calculated by the following equation:[1-3]

$$D^{Li^+} = \frac{4}{\pi}\left(\frac{mVM}{MA}\right)^2\left(\frac{\Delta Es}{\tau(dE\tau/d\sqrt{\tau})}\right)^2\left(\frac{\tau << L^2}{DLi^+}\right) \quad (1)$$

In this formula, m and M represent the mass and molecular weight of $Li[Li_{0.21}Ni_{0.131}Co_{0.122}Mn_{0.538}]O_2$, respectively. V_M is the molar volume of the compound and can be deduced from the crystallographic data. L is the radius of the active particle, and A is the active surface of the electrode based on the result of the BET test. If the relationship of potential (E) and the square root of time ($\tau^{1/2}$) exhibits a behavior of beeline across the whole time period, as shown in the inset curves in Fig. 10a-b, the equation 1 can be simplified as:[1-3]

$$D^{Li^+} = \frac{4}{\pi}\left(\frac{mVM}{MA}\right)^2\left(\frac{\Delta Es}{\Delta E\tau}\right)^2 \quad (2)$$

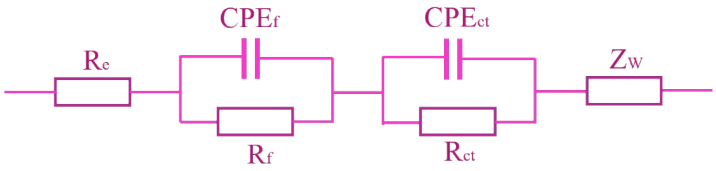

Fig. S13 Equivalent circuit for the Nyquist plots.

Table S4. The impedance parameters of NM-LRM and PD-LRM samples after cycle.

NM-LRM	R_s	R_f	R_{ct}
5th	14.36	25.74	46.09
20th	15.76	29.02	107.1
40th	16.7	30.3	161.2
60th	17.04	32.8	238.6
80th	17.39	34.5	301.9
100th	19.29	35.42	338.7

PD-LRM	R_s	R_f	R_{ct}
5th	10.83	20.74	38.68
20th	11.64	22.63	46.38
40th	12.2	24.67	50.88
60th	12.83	25.99	70.99
80th	13.26	26.75	88.43
100th	13.7	27.2	112.5

References

1 X. H. Rui, N. Ding, J. Liu, C. Li and C. H. Chen, *Electrochim. Acta,* 2010, **55,** 2384-2390.

2 K. M. Shaju, G. V. Subba Rao and B. V. R. Chowdari, *J. Mater. Chem.,* 2003, **13,** 106-113.

3 Y. Q. Qiao, J. P. Tu, X. L. Wang, J. Zhang, Y. X. Yu and C. D. Gu, *J. Phys. Chem. C,* 2011, **115,** 25508-25518.